SYNTHESIS, CHARACTERIZATION, THERMAL BEHAVIOR AND ANTIMICROBIAL ACTIVITY OF 3-METHYL BENZOATE COMPLEXES OF TRANSITION METAL WITH HYDRAZINE

S. Mohanapriya[1], Muthukumaran[2] and S. Vairam[3*]

[1]Department of Chemistry, Tamilnadu College of Engineering, Coimbatore, India
[2]Department of Biotechnology, Government College of Technology, Coimbatore, India
[3]Department of Chemistry, Government College of Technology, Coimbatore, India

ABSTRACT. Reaction of the ligands, 3-methyl benzoic acid (mbH) and hydrazine with transition metal ions form the complexes of formulae, $[M(N_2H_4)_2(mb)_2].H_2O$ where M = Co(II) and Zn(II) at pH = 5-6, $[M(N_2H_4)_n(mb)_2].xH_2O$ where M = Ni(II), n = 2, x = 0 at pH = 5 and M = Cd, n = 1, x = 1 at pH = 6. The same acid also forms metal carboxylates with zinc and copper of formula, $[Zn(mb)_2H_2O].H_2O$ at pH = 6 and $[Cu(mb)_2].H_2O$ at pH = 5, respectively. The IR spectra of the complexes show that hydrazine is present as bridging bidentate ligand and the carboxylic acid as monodentate bridging carboxylate anion. The electronic spectra, magnetic moments and ESR spectral data suggest the coordination number. Thermal studies show that cobalt, zinc and nickel complexes containing hydrazine, and carboxylates of copper, zinc on their thermal decomposition form the corresponding metal oxides in nano size in the temperature range 755-815 °C. The antibacterial and antifungal activity show that both activities of the complexes are higher than that of the acid and among the complexes, cadmium compound shows more antimicrobial activity towards bacteria and fungi.

KEY WORDS: Hydrazinium complexes, 3-Methyl benzoic acid, Thermal analysis, IR, Electronic spectra, Biological activity

INTRODUCTION

m-Toluic acid is an important chemical intermediate and is widely used to prepare insect repellents, polymer film former and thermal stabilizers for PVC. Benzoic acid is known to have antibacterial and antifungal properties. Aromatic carboxylic acids are widely used in medicine as non-steroidal anti-inflammatory drugs, e.g. ibuprofen, naproxen, diclophenac and fenclofenac [1-4]. Ibuprofen was the first member of propionic acid derivatives to be introduced in 1969. Ibuprofen is effective in reducing high body temperature, and an anti-inflammatory which inhibits normal platelet function. It is used for joint and muscle pain than other pain killer and has been used by people for arthritis for years. However, it can cause gastrointestinal upset and bleeding [5]. Naproxen is chemically (S)-6-methoxy-α-methyl-2-naphthalene acetic acid as sodium salt. It is a non-steroidal anti-inflammatory drug commonly used for the reduction of moderate to severe pain, fever, inflammation and stiffness [6]. Diclofenac, a drug, causes an asymptomatic increase of plasma transaminase in patients, and life-threatening fluminant hepatitis is induced in a very small percentage [7]. The molecular mechanisms of liver injury are largely unknown [8]. Fenclofenac, another non-steroidal anti-inflammatory drug, is a weak organic acid used in rheumatism. It has a dose related simulator effect on the depressed body weight gain which is a feature of adjuvant disease [9].

Benzoic acid is used in combination with salicylic acid in dermatology as a fungicidal treatment for fugal skin diseases [10]. It can be found in cosmetics, deodorants and toothpastes [11-13]. Benzoic acid and its salts are used to preserve food from growth of microorganism and it can be found in beverages, fruit products, chemically leavened baked goods and drink industry [14-17]. The carboxylic group is available for interaction with metals which can have synergistic or antagonistic effect to the biological activity. It was found that anti-inflammatory

_____
*Corresponding author. E-mail: vamshen@yahoo.com

and anti-bacterial activity of metal complexes was higher than that of the parent carboxylic acids [18]. The anti-bacterial effect of some drugs could be enhanced when they are chelated to a metal [19]. The benzoate group as a substituent serves as a site to complex targeting group that can aid in the delivery of the compound to bacteria cell in the body [20]. The design and synthesis of transition metal complexes with carboxylate ligands have been received a considerable interest in coordination chemistry, due to the fact that this type of complexes has potential applications in molecular based magnets, catalysis, supra molecular chemistry and biological systems [21-22]. The carboxylate anion can adopt a wide range of bonding modes (monodentate symmetric and asymmetric chelating and bidentate and monodentate bridging) [23]. In addition, hydrogen bonding plays an important role in bioinorganic chemistry and is a gateway to molecular organization [24]. The literature survey of the past few years reveals the fact that a significant development in the field of biological activity of metal chelates plays a vital role in the case and treatment of cancer [25-28]. The complexes of transition metals like Co, Ni and Cu are influenced by various physiochemical parameters. The clear understanding of structure and spectroscopic properties of metal complexes usable for their biological applications is the aim of present work. The present work deals with the synthesis and characterization of Co, Ni, Cd, Zn and Cu(II) complexes of 3-methyl benzoic acid with/without hydrazine.

EXPERIMENTAL

The chemicals and solvents used were of AR grade received from Fluka Chemicals. The double distilled water was used for the preparation and chemical analyses. Hydrazine hydrate 99.99% pure was used as received.

Preparation of $[M(N_2H_4)_n(mb)_2].xH_2O$ where M = Co , Zn n = 2 and x = 1; M = Ni, n = 2 and x = 0; M = Cd, n = 1 and x = 1

These complexes were prepared by dissolving corresponding metal nitrate (1 mmol, for example $Co(NO_3)_2 .6H_2O$; 0.2910 g in 20 mL of distilled water) and poured to ligand solution which was prepared by mixing 3-methyl benzoic acid (2 mmol, 0.2720 g) and hydrazine hydrate (4 mmol, 0.2 mL) in 60 mL hot water with constant stirring. In all the cases, clear solutions obtained initially, became turbid after 30 min when stirred using a magnetic stirrer at 50 °C and changed to micro crystalline solids when left undisturbed. The colors of the crystals were pink and pale violet for cobalt and nickel, respectively, and colorless for zinc and cadmium. Zinc hydrazine complex was formed only in 1:1 alcohol medium at pH = 5. The solution with products were cooled, filtered and washed with distilled water, ethanol and then with ether. Then they were dried in desiccators containing anhydrous $CaCl_2$.

Preparation of $[Zn(mb)_2.H_2O].H_2O$ and $[Cu(mb)_2].H_2O$

These compounds were prepared by adopting similar procedure as mentioned above. While adding an aqueous solution of 3-methyl benzoic acid (2 mmol, 0.2720 g in 40 mL hot water) with metal nitrate solution 1 mmol in 20 mL of distilled water. The above solution mixture which appeared cloudy at first, changed to micro crystalline solid (pale green for copper at pH = 5, and colorless for zinc at pH = 6) after the addition of ligand to metal solution. The above solution was mixed thoroughly using magnetic stirrer for 30 min to make completion of precipitation at 50 °C. The products were separated by filtering and washed appropriately and dried.

Antimicrobial activity

Anti-bacterial and anti-fungal activities of the synthesized metal complexes were performed using well diffusion assay [29]. Bacterial (*Escherichia coli*, *Staphylococcus aureus*, *Salmonelle*

paratyphi, *Bacillus substilis*) and fungal strains (*Candida albicans*, *Aspergillus niger*, *Aspergillus fumigate)* were used as test organisms in this study. For antibacterial activity, 36 g of Muller Hinton media was mixed with 100 mL of distilled water and autoclave at 15 psi for 15 min. The sterilized media were poured into Petri dishes and the solidified plates were bored with 6 mm cork borer. Four wells were made in each Petri plate and 20 µL (20 µg) of metal hydrazine complex solution was added to two wells and 20 µL of distilled water (control) was added to other wells. The plates were incubated at 37±2 ºC for 24 h and observed for zone of clearance around the wells.

For anti-fungal activity, pore suspensions, 0.5 mL (10^{-6}-10^{-7} Spore/mL) of each of the investigated organisms (*Candida albicans*, *Aspergillus niger*, *Aspergillus fumigate*) was added to sterile agar medium just before solidification, then poured into sterile Petri dishes (9 cm in diameter) and left to solidify. Using sterile cork borer (6 mm in diameter), four holes (wells) were made in each dish and then 20 µL of the tested compounds dissolved in water (100 mg/mL) were poured into these holes. Finally, the dishes were incubated at 37 ºC for 48 h where clear inhibition zones were detected around each hole. The experiment was carried out with a blank under the same condition for each organism and by subtracting the diameter of inhibition zone of the blank from that obtained in each case. Anti-bacterial and anti-fungal activities are a mean of three replicates [29].

In vitro cytotoxicity

MTT cell proliferation assay was employed to estimate the cytotoxicity of synthesized metal complex [30]. Vero cell line was purchased from NCCS (National Center for Cell Sciences) Pune, India used for MTT assay. The cell lines were maintained at 37 ºC, 5% CO_2, 95% air and 100% relative humidity. The mono layer cells were detached by Trpsin treatment to make single cell suspensions and diluted to final density of 1×10^5 cells/mL using 5% FBS. One hundred micro liters per well for cell suspensions were sealed into 96 well plates. After 48 h of incubation, 15 µL of MTT (5 mg/mL) in phosphate buffered saline (PBS) was added to each well and incubated at 37 ºC for 4 h. The samples from were solubilized in 100 µL of DMSO and the absorbance was measured at 570 nm. Cell viability, the ratio (expressed as a percentage) of absorbance of treated cells to untreated cells, was calculated with respect to control using the relation: % cell viability = [test absorbance]/[control absorbance] × 100.

Physico chemical techniques

The composition of the complexes were fixed by chemical analysis and confirmed by micro elemental analysis. Hydrazine content was determined by titrating against standard KIO_3 (0.025 mol L^{-1}) under Andrew's conditions [31]. Metal content was determined by titrating with EDTA (0.025 mol L^{-1}) after decomposition the complexes with 1:1 nitric acid [31].

IR spectra of the complexes in the region 4000-400 cm^{-1} were recorded as KBr pellets using a Perkin Elmer 597 spectrophotometer. Electronic reflectance spectra for the solid state complexes were obtained using a Jasco U 530 UV-Visible spectrometers by dispersing the solid samples in nujol mull. The magnetic susceptibility of the complexes was measured using a vibrating sample magnetometer, VSM EG&G model 155 at room temperature and the data were corrected for diamagnetism. The X-ray powder patterns of the complexes were recorded using a Siemens D-5005 X Ray diffractometer and JEOL FDX 8P X-ray diffraction using Cu K_α Nickel filter. The simultaneous TG-DTA experiments were carried out using STA 1500 thermal analyzers, NETZSCH-Geratebeau Gmbh thermal analyzer and the curves obtained in air at the heating rate of 10 ºC min^{-1} using 5 to 10 mg of the samples. Platinum cups were employed as sample holders and alumina as reference. The temperature range was ambient to 900 ºC.

RESULTS AND DISCUSSION

Electronic spectra, magnetic susceptibility and ESR spectra

The complexes were sparingly soluble in water and organic solvents, the electronic reflectance spectra were recorded in solid state.

The band appear in the range 11787 and 26880 cm^{-1} are assigned to the $4A_{2g}$ and $4T_{1g}(P)$ states of typical six coordinated Co(II) complex. The corresponding nickel complex shows peak at 11850 and 14757, 23790 cm^{-1} which are ascribed to $3T_{2g}$, $3T_{1g}$ and $3T_{1g}$ (P) transitions respectively of octahedral geometry of Ni(II) [32]. The copper carboxylate shows bands in the region, 11585 and 26340 cm^{-1}, respectively, evidence the tetrahedral geometry of Cu(II) [33]. The axial ESR spectrum for copper carboxylate shown in Figure 1 has features at g $_{ll}$ and g$\perp$ = 2.069 which clearly indicates that the copper(II) ion is in isotropic indicating a tetrahedral geometry with coordination number 4. The magnetic moment values obtained for the cobalt, nickel and copper carboxylate complexes 3.10, 2.04 and 1.74 BM, respectively, support the geometry of the complexes.
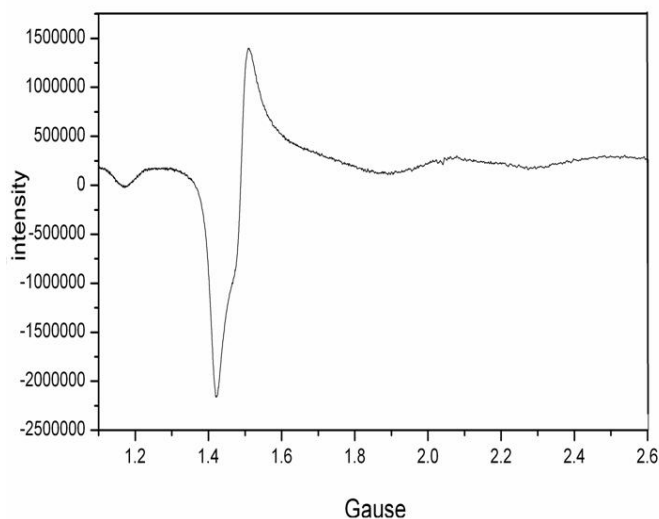

Figure 1. ESR spectrum of [Cu(mb}$_2$].H$_2$O.

IR spectra of complexes

The analytical and IR spectral data of the complexes are summarized in Table 1 and 2. All the hydrated complexes, except nickel hydrazine complexes show a broad band in the region 3520-3302 cm^{-1} which is assigned to v $_{OH}$ vibrations of associated water molecules. An additional sharp peak in the region of 540-578 cm^{-1} appearing in the spectra of Co, Zn, Cd hydrazine and Cu, Zn carboxylate complexes supports the presence of lattice water molecules. In the case of Zn carboxylate, an additional band observed at 848 cm^{-1} due to the presence of coordinated water molecule [34]. The hydrazine complexes of cobalt, zinc, nickel and cadmium hydrazine complexes show N-N stretching frequency in the range 964-979 cm^{-1} indicating bidentate bridging nature of hydrazine [35]. The entire hydrazine complex shows N-H stretching frequency range 3248-3302 cm^{-1}. The asymmetric and symmetric stretching frequencies of carboxylate ions are seen in the range 1612-1597 cm^{-1} and 1404 -1296 cm^{-1}, respectively, with a difference ($\Delta v_{asym - sym}$) of 144-223 cm^{-1} indicating the monodentate linkage of carboxylate group

[34]. The IR spectrum of pure acid shows absorption at 1682 cm^{-1} corresponding to free COOH group. All the complexes show the sharp peak at the frequency range of 470-509 cm^{-1} which is ascribed to the characteristic vibration of M-O bond [36].

Table 1. Analytical data of the complexes.

Compound	Elemental analysis found (cald) %			N$_2$H$_4$ found (cald)%	Metal found (cald)%	D. pt.	Yield %	Color
	C	H	N					
[Co(N$_2$H$_4$)$_2$(mb)$_2$].H$_2$O	45.52 (46.68)	5.68 (5.83)	13.57 (13.61)	15.50 (15.56)	14.20 (14.33)	229	79	Pink
[Zn(N$_2$H$_4$)$_2$(mb)$_2$].H$_2$O	45.80 (45.91)	5.68 (5.73)	13.20 (13.39)	15.20 (15.30)	15.50 (15.70)	218	84	White
[Ni(N$_2$H$_4$)$_2$(mb)$_2$]	48.52 (48.86)	5.68 (5.59)	13.87 (14.25)	16.13 (16.20)	14.70 (14.80)	248	80	Violet
[Cd(N$_2$H$_4$)(mb)$_2$].H$_2$O	44.18 (44.38)	4.48 (4.62)	6.33 (6.47)	6.33 (6.47)	25.87 (25.98)	209	89	White
[Cu(mb)$_2$]H$_2$O	53.12 (54.57)	4.38 (4.54)	-	-	17.28 (18.06)	189	82	Light green
[Zn (mb)$_2$H$_2$O].H$_2$O	50.80 (51.33)	4.64 (4.81)	-	-	17.48 (17.56)	100	77	White

cald - calculated, D. Pt. - decomposition point.

Table 2. IR data of the complexes.

Compound	Frequency (cm^{-1})
[Co(N$_2$H$_4$)$_2$(mb)$_2$].H$_2$O	3520(br), 3302 (s), 1551(br),1401(s), 972(s),555(s), 509(s), 144
[Zn(N$_2$H$_4$)$_2$(mb)$_2$].H$_2$O	3520(m), 3302 (s), 1551(br),1374(s), 972(s),555(s), 486(s), 177
[Ni(N$_2$H$_4$)$_2$(mb)$_2$]	3302(br),1604(b),1381(s), 979(s), 486(s), 223
[Cd (N$_2$H$_4$)(mb)$_2$].H$_2$O	3448(m), 3248 (s), 1612(br),1396(s), 964(s),578(s), 486(s), 216
[Cu(mb)$_2$]H$_2$O	3448(br), 1597(b),1404(s), 563(s), 493(s), 193
[Zn (mb)$_2$H$_2$O].H$_2$O	3520(m), 1604(b),1404(s), 848(s), 540(s), 470(s), 200

br – broad, s – sharp, m – medium.

Thermal analysis

Thermal degradation is an important tool for coordination compounds to derive many conclusions about their nature and thermal stability. Especially the nature and number of water molecules present in the hydrated complexes may be deduced on the basis of the temperature range at which it is eliminated. The thermal data of the complexes are listed in Table 3. The compositions of the intermediates and the final products are those, which fit with the observed mass losses in TG. Thermo gravimetric results are in good agreement with the DTA data. The corresponding TG-DTA graphs are shown in Figure 2a-f.

The complexes, owing to the possessing of similar formulae, cobalt and zinc complexes show similar thermal degradation patterns as revealed by their TG-DTA curves shown in Figure 2a and 2d. The TG curves of cobalt and zinc complexes show mass losses 18.6–19.5% in the first step implying removal of water and hydrazine. In the DTA, the above loss is accompanied by two endothermic at 229 and 250 °C for cobalt complex and endo followed by exothermic at 218 and 244 °C, respectively, in the case of zinc complex. Next step in Co complex is the decomposition of respective carboxylate to metal oxide via the corresponding metal carbonate. This observation is supported by their mass losses and endothermic around 485 °C. In the case of zinc complex, the decomposition of respective carboxylate to metal carbonate via the corresponding metal acetate. This observation is revealed by their mass loss and exotherm in DTA around 474 °C and confirmed by the decomposition point of acetate [37]. The last step in this decomposition, is found to be formation of corresponding metal oxide.

Table 3. Thermal data of the complexes.

| Complex | DTA Temp°c | Thermogravimetry | | | Nature of Decomposition |
| | | Temp range | Weight loss% | | |
			Obsd.	Cald.	
[Co (N$_2$H$_4$)$_2$ (mb)$_2$].H$_2$O	229 (+) 250(-) 419(-)	200-435	18.6	19.9	Dehydration and dehydrazination
	485(+)	436 -545	69.9	71.1	Decomposition to CoCO$_3$
	692(+) 815(-)	545-900	79.7	80.5	Decomposition to Co$_3$O$_4$
[Zn(N$_2$H$_4$)$_2$ (mb)$_2$].H$_2$O	218(+) 244(-)	200-260	19.5	19.6	Dehydration & dehydrazination
	474(-)	261-500	43.9	44.0	Decomposition to zinc acetate
	577(-)	501-600	69.8	69.9	Decomposition toZnCO$_3$
	785(-)	601-900	82.4	82.4	Decomposition to ZnO
[Ni(N$_2$H$_4$)$_2$ (mb)$_2$]	248(-) 259(-) 385(+) 442(-)	200-450	75.0	76.4	Decomposition to nickel benzoate
	811(+) 833(-)	451-900	83.0	83.0	Decomposition to NiO
[Cd (N$_2$H$_4$) (mb)$_2$].H$_2$O	209(+) 231(+) 397(+)	200-400	11.5	11.6	Dehydration & dehydrazination
	485(-) 522(+)	401-550	53.2	53.3	Decomposition to cadmium acetate
	562(+) 581(-)	551-900	60.1	60.1	Decomposition to CdCO$_3$
[Cu (mb)$_2$] H$_2$O	189(+)	150-200	5.1	5.11	Dehydration
	215(+) 230(+) 581(-)	201-250	13.1	13.1	Decomposition to Copper benzoate
	800(+)	601-900	77.3	77.4	Decomposition to CuO
[Zn (mb)$_2$ H$_2$O].H$_2$O	100(+) 140(-) 185(-)	50-300	15.7	15.8	Dehydration
	350(-) 600(-)	301-600	38.0	38.0	Decomposition to zinc carbonate
	811(+)	601-900	59.7	59.8	Decomposition to zinc oxide

(+) = Endothermic peak, (-) = Exothermic peak, Obsd = Obseved, Cald = Calculated, DTA = Differencial thermal analysis

In the case of Ni complex, exothermic dehydrazination occurs at 248 °C. Subsequently a sudden decomposition occurs showing endotherm followed by exotherm at 385 °C and 442 °C respectively, to form nickel benzoate which again decomposes to form NiO showing an endotherm at 811 °C. The decomposition point of nickel benzoate matches with the reported value [38].

In the case of cadmium complex, its TGA reveals three steps decomposition. Dehydration takes place in the first step, exhibiting two endotherm at 209 and 231 °C (Figure 2d). The second step is the formation of metal acetate, with a display of an one exothermic and one endothermic peak at 485 and 522 °C in DTA. Next step is the decomposition of respective acetate to metal carbonate. This observation is supported by their mass losses and one exotherm and one endotherm at 581 and 562 °C. The final product is carbonate as evidenced by the decomposition shown in the DTA curve matching with the reported values [39].
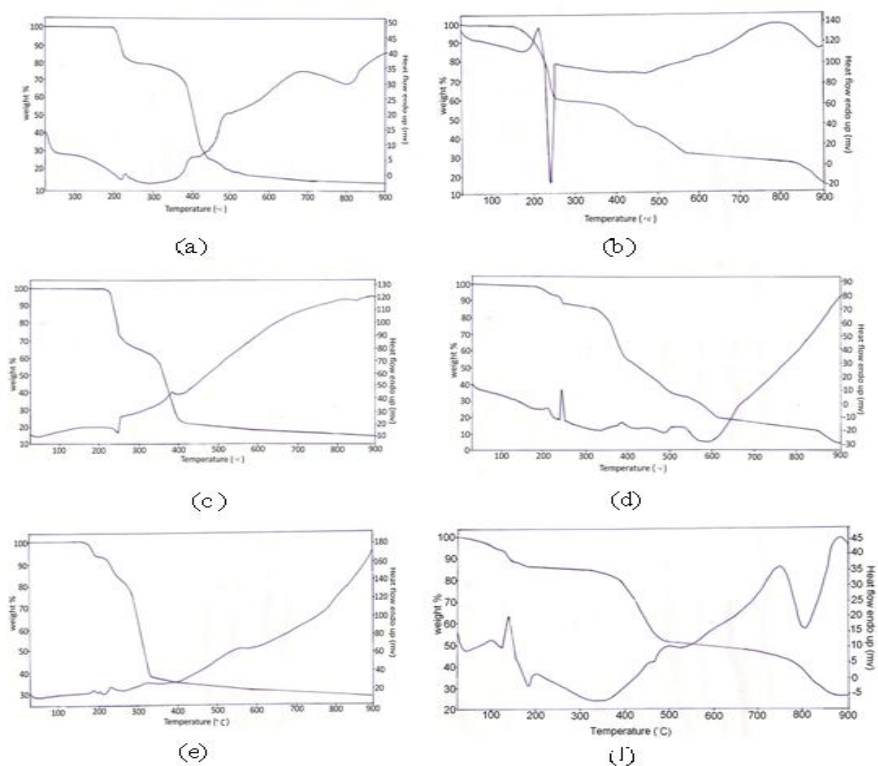
Figure 2. TG-DTA of **(a)** $[Co(N_2H_4)_2(mb)_2].H_2O$, (b) $[Zn(N_2H_4)_2(mb)_2].H_2O$, (c) $[Ni(N_2H_4)_2(mb)_2]$, (d)$[Cd(N_2H_4)(mb)_2].H_2O$, (e) $[Cu(mb)_2].H_2O$ and (f) $[Zn(mb)_2H_2O].H_2O$.
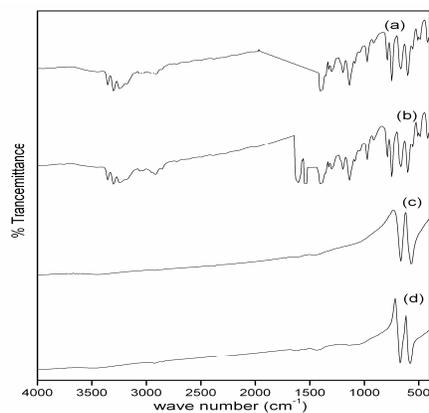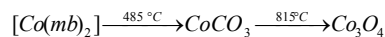

Figure 3. IR spectra of intermediate residue in TG-DTA (a) $[Co(N_2H_4)_2(mb)_2].H_2O$, (b) Dehydration and dehydrazination, (c) Decomposition to $CoCO_3$ and (d) decomposition to Co_3O_4.

In order to follow the degradation patterns, IR data for intermediate of each step of decomposition of cobalt complex were collected and compared with the IR of known compounds. It is interesting to note the absence of peak around 972 cm^{-1} corresponding to N-N stretching and series of peaks from 3302-3520 cm^{-1} due to N–H and O–H in the IR spectrum (Figure 3) which clearly says that N_2H_4 and H_2O were removed due to decomposition. In addition, spectra of the carbonate produced during decomposition shown in Figure 3c are also comparable with that of anhydrous cobalt carbonate.

Comparing the thermograms of Cu and Zn carboxylates, it is understood that they have similar composition and comparable appearences of their TG curves but with different temperature ranges in TG and DTA. In these complexes also, water is removed in the range 100-189 °C. Subsequently, copper carboxylate decomposes completely to copper oxide via copper acetate and copper carbonate. Zinc carboxylate decomposes completely to zinc oxide via zinc carbonate.

The scheme of decomposition of complexes is shown below.

I $[M(N_2H_4)_n(mb)_2]H_2O \xrightarrow[\substack{(H_2O \& N_2H_4)}]{209-229°C} [Zn(mb)_2]$

  where M = Co, Zn , n = 2 and Cd, n = 1

II $[Ni(N_2H_4)_n(mb)_2] \xrightarrow[\substack{(-N_2H_4)}]{385-400°C} Ni\ (C_6H_5COO)_2 \xrightarrow{811°C} NiO$

III $[M(mb)_2] \xrightarrow{577\ °C} ZnCO_3 \xrightarrow{785°C} ZnO$

  $[Co(mb)_2] \xrightarrow{485\ °C} CoCO_3 \xrightarrow{815°C} Co_3O_4$

  $[Cd(mb)_2] \xrightarrow{485\ °C} Cd(CH_3COO)_2 \xrightarrow{581°C} CdCO_3$

Metal carboxylate

$[Cu(mb)_2]H_2O \xrightarrow[\substack{(-H_2O)}]{189°C} Cu(C_6H_5COO)_2 \xrightarrow{518\ °C} CuCO_3 \xrightarrow{800\ °C} CuO$

$[Zn(mb)_2.H_2O]H_2O \xrightarrow[\substack{(-2H_2O)}]{100-185°C} [Zn(mb)_2] \xrightarrow{459°C} ZnCO_3 \xrightarrow{811°C} ZnO$
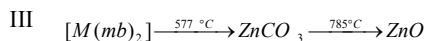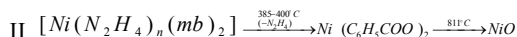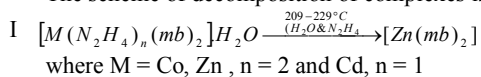
SEM studies

Owing to the evolution of various gases from hydrazine and carboxylate moiety of the complexes, it is generally observed that the hydrazinated metal carboxlylates yield metal oxides on thermal decomposition, in the micro to nano scale. In the case of the complexes reported here, it is found that they result in metal oxides in cluster form containing nano scale particles, when there were calcined at their decomposition temperature followed by sintering at the same temperature. The SEM images of metal oxides formed from the decomposition of complexes are shown in Figure 4. The size of the particals is in the range of 49–149 nm, implying that the complexes may be used as a precursors for nanometal oxides [40]. This observation is further substantiated by its XRD pattern of ZnO (Figure 5) matching with the standard pattern reported (JCPDS card no. 361451). The XRD pattern of oxide residue shows matching peaks at 100, 002, 101, 103 and 112 (Figure 5). The other peaks may be due to impurity resulting from oxidation of organic moiety of the complexes. Further, size of particals of ZnO is worked out to be in nano scale, using Scherrer's formula [41] D = Kλ/β cosθ, where λ is the X-ray wavelength, β is the full width of height maximum (FWHM) of a diffraction peak, θ is the diffraction angle, and K is Scherer's constant of the order of 0.89.

Antimicrobial activity

The anti-bacterial and anti-fungal activities of the synthesized compounds were tested against various bacteria like *Escherichia coli*, *Staphylococcus aureus*, *Salmonelle paratyphi*, *Bacillus*

substilis and fungus namely *Candida albicans*, *Aspergillus niger*, *Aspergillus fumigate*. The inhibition zone of the compounds against the growth of microorganisms are summarized in Table 4. The Co(II), Zn(II), Ni(II) complexes show inhibition against *Escherichia coli*, *Staphylococcus aureus*, *Salmonelle paratyphi*, *Bacillus substilis*, *Candida albicans*, *Aspergillus niger*, *Aspergillus fumigate*. Of all the complexes, Cd(II) complex shows greater inhibition against *Bacillus substilis* followed by *Salmonelle paratyphi*. Similarly in fungus *Candida albicans*, *Aspergillus niger* followed by *Aspergillus fumigate* and moderate inhibition against *Escherichia coli*, and *Staphylococcus aureus*.
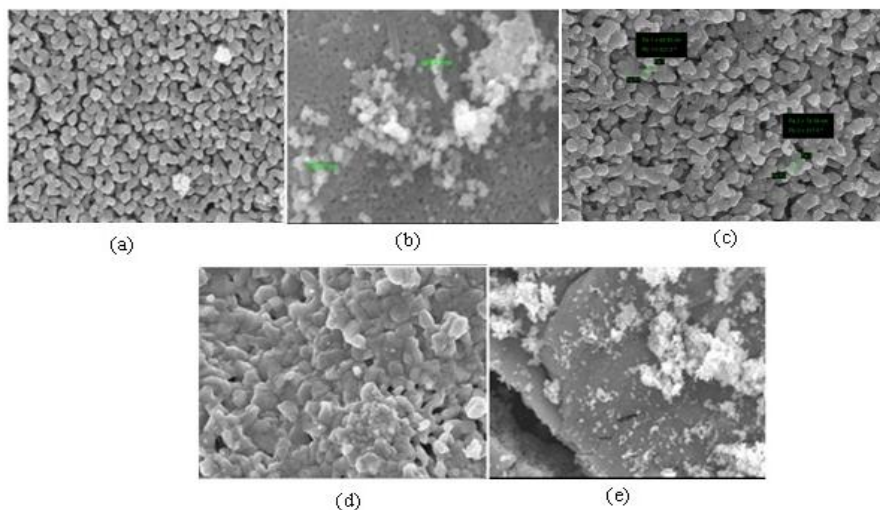

Figure 4. SEM images of metal oxide obtained from (a) $[Co(N_2H_4)_2(mb)_2].H_2O$, (b) $[Zn(N_2H_4)_2(mb)_2].H_2O$, (c) $[Ni(N_2H_4)_2(mb)_2]$, (d) $[Cu(mb)_2].H_2O$ and (e) $[Zn(mb)_2 H_2O].H_2O$.

A comparative study of the ligand and complexes indicates that the complexes exhibited higher antimicrobial activity then the free ligand. Such increased activity of the complexes can be explained on the basis of overtone's concept [42] and chelation theory [43]. These complexes hinder the respiration process of the cell and thus block the synthesis of the proteins, restricting further growth of the organism. Moreover, the chelating nature of the metal complex enhances the lipophilic property making the complex penetrate through bacterial lipid membrane [44]. According to overtone's concept of cell permeability, passage of metal complexes causing lipid solubility is a critical factor in antimicrobial activity [45]. The decrease in polarity of metal ion attributes to ligand orbital overlap and sharing of positive charge with the donor groups increases the hydrophobicity index of the hydrazine metal complex which further enhances its penetration into lipid membrane leading to cell death as stated. The antimicrobial property of synthesized metal complex makes them as a potential candidate for medical and biological applications.

The cytotoxicity of the metal complex on *in vitro* vero cell lines is shown in Figure 6. The results revealed that the cell viability was decreased in dose dependent manner. The maximum cell viability of 70.96% was observed at 30 µg/mL dosage of metal complex. The cytotoxicity assay showed that low level of metal complex not affected the normal cell lines and has significant inhibition at higher levels. Thus, the synthesized metal complex can be used as an effective antimicrobial agent with less effect on normal cell lines at low levels.
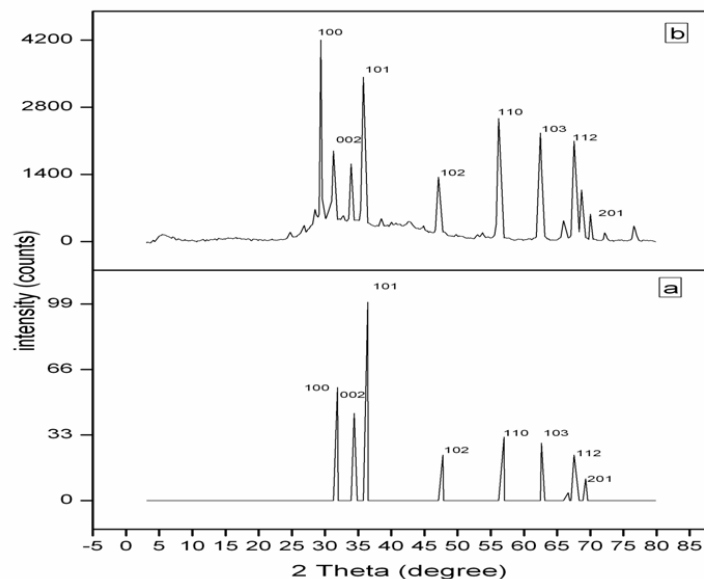
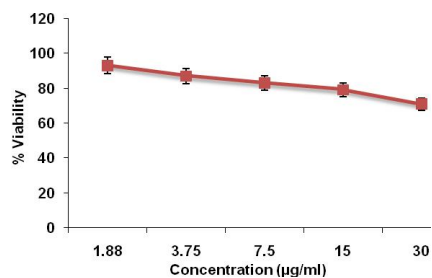Figure 5. Powder XRD patterns of (a) standard ZnO (JCPDS) and (b) residual ZnO.

Figure 6. *In vitro* cytoxicity of cadmium hydrazine complex with normal cell.

Table 4. Antimicrobial activity of the complexes.

Complex	Inhibition zone (mm)						
	Escherichia coli	Staphylococus aureus	Salmonelle paratyphi	Bacillus substilis	Candida albicans	Aspergillus niger	Aspergillus fumigate
$[Co(N_2H_4)_2(mb)_2].H_2O$	6	5	7	8	7	8	7
$[Zn(N_2H_4)_2(mb)_2].H_2O$	7	7	8	7	6	7	7
$[Ni(N_2H_4)_2(mb)_2]$	8	8	7	7	7	5	5
$[Cd(N_2H_4)(mb)_2].H_2O$	8	7	14	15	21	20	20
$[Cu(mb)_2].H_2O$	7	6	7	7	5	6	6
$[Zn(mb)_2 H_2O].H_2O$	8	7	6	6	5	5	5

CONCLUSION

The 3-methyl benzoic acid and hydrazine hydrate yield the complexes of formulae, $[M(N_2H_4)_2(mb)_2].H_2O$ where M = Co(II) and Zn(II) at pH = 5-6 and $[M(N_2H_4)_n(mb)_2].xH_2O$

where M = Ni (II), n = 2, x = 0 at pH = 5 and M = Cd, n = 1, x = 1 at pH = 6. The same acid also forms metal carboxylates with zinc and copper of formula, $[Zn(mb)_2H_2O].H_2O$ at pH = 6 and $[Cu(mb)_2].H_2O$ at pH = 5. The composition of the complexes was confirmed by elemental data. The complexes are sparingly soluble in water due to polymeric nature. The IR frequencies reveal the coordination of the hydrazine with metal and the coordination mode of carboxylate ion to metal. The thermal data reveals that various steps of decomposition of the complexes to form their metal oxide and metal carbonate as final products. The electronic spectra and the magnetic susceptibility values reveal the geometry of Co and Ni complexes. They may have distorted octahedral geometry with coordination number 6 (Figure 7). The ESR spectrum of copper carboxylate implies that the complex has tetrahedral geometry. However, these structures can be confirmed by single crystal XRD only. The SEM studies reveal the presence of respective metal oxides. The antimicrobial property of our synthesized metal complex makes them as a potential candidate for medical and biological applications. The metal complexes may be used as an effective antimicrobial agent with less effect to normal cells at low levels.
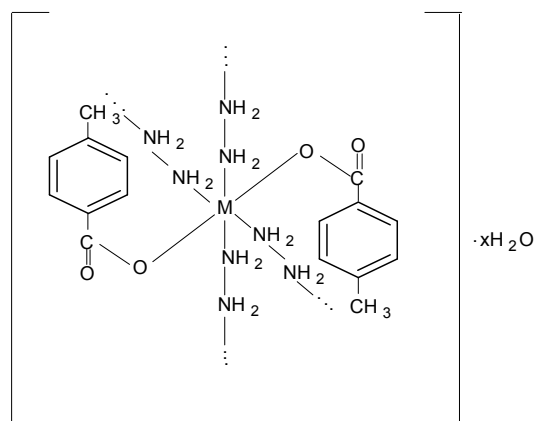

Figure 7. Proposed structure of $[M(N_2H_4)_2(mb)_2].H_2O$, where M = Co and   x = 1,   M = Ni, x = 0.

REFERENCES

1. Emery, P.; Kong, S.X.; Ehrich, E.W.; Watson, D.J.; Towheed, T.E. *Clin. Ther.* **2002**, 24, 1225.
2. Sorenson, J.R.J. *Anti-inflammatory activities of copper complexes* in *Metal Ions in Biological Systems*, Sigel, H. (Ed.), Vol. 14, Marcel Dekker: New York; **1982**, p 77.
3. Dendrinou-Samara, C.; Tsotsou, G.; Ekateriniadou, L.V.; Kortsaris, A.H,; Raptopoulou, C.P.; Terzis, A.; Kyriakidis, D.A.; Kessissoglou, D.P. *J. Inorg. Biochem.* **1998**, 71, 171.
4. Stuhlmeier, K.M.; Li, H.; Kao, J.J. *Biochem. Pharmacol.* **1999**, 57, 313.
5. Riley, T.R.; Smith, J.P. *Am. J. Gastroenterol.* **1998**, 93, 1563.
6. Tirumala Rao, K.; Vaikunta Rao, L. *Am. J. Anal. Chem.* **2013**, 4, 286.
7. Bhogaraju, A.; Nazeer, S.; AL-Baghdadi, Y.; Rahman, M.; Wrestler, F.; Patel, N. *South. Med. J.* **1999**, 92, 711.
8. Purcell, P.; Henry, D.; Melville, G. *Gut.* **1991**, 32, 1381.
9. Atkinson, T.C.; Green, D.C.; Leach, E.C. *Proc. Royal Soc. Med.* **1977**, 70 1.
10. Becker, C.; Dressman, J.B.; Amidon, G.L.; Junginger, H.E.; Kopp, S.; Midha, K.K.; Shah, V.P.; Stavchansky, S.; Barends, D.M. *J. Pharm. Sci.* **2008**, 97, 3709.

11**.** Diehl, K.B. *Am. Fam. Physician.* **1996**, 54, 1687.

12. Abrahamsen, T.G.; Widing, E.; Glomstein, A.; Gaustad, P. *J. Infect. Dis.* **1992**, 24, 391.

13. Rastogi, S.C.; Lepoittevin, J.P.; Johansen, J.D.; Frosch, P.J.; Menne, T.; Bruze, M.; Dreier, B. Andersen, K.E.; White, I.R. *Contact Dermatitis* **1998**, 39, 293.

14. Sainio, E.; Kanerva, L. *Contact Dermatitis* **1995**, 33, 100.

15. Hanssen, M. *E for additives: The Complete E Number Guide*, Maurice, Thorsons, Harper Collins Publishers: UK; 1984.

16. Dock, L.L.; Floros, J.D.; Linton, R.H. *J. Food Prot.* **2000**, 63, 1026.

17. Islam, M.; Chen, J.; Doyle, M.P.; Chinnan, M. *J. Food Prot.* **2002**, 65, 1411.

18. World Health Organisation *International Programme on Chemical Safety*, Concise International Chemical Assessment Document No. 26, Geneva, **2000**.

19. Sorenson, J.R.J.; Kishore, V.; Pezeshk, A.; Oberley, L.W.; Leuthauser, S.W.C.; Oberley, T.D. *Inorg. Chim. Acta* **1984**, 91, 285.

20. Chohan, Z.H.; Sherazi, S.K.A. *Metal Chelates Metal-Based Drugs* **1997**, 4, 327.

21. Amanda, R. K.; Matthew, J. P.; Doug, A. M.; Brian, D. W.; Claire, A. T.; Wiley, J. Y. *Inorganica Chimica Acta.* **2010,** 364, 125.

22. Rardin, R. L.; Tolman, W. B.; Lippard, S. J. *New J. Chem.* **1991**, 15, 417.

23. Holm, R.H.; Kennepohl, P.; Solomon, E.I. *Chem. Rev.* **1996**, 96, 2239.

24. Rardin, R.L.; Bino, A.; Poganiuch, P.; Tolman, W.B.; Liu, S.; Lippard S.J. *Angew. Chem., Int. Ed. Engl.* **1990**, 29, 812.

25. Busch, D.H.; Stephenson, N.A. *Coord. Chem. Rev.* **1990**, 100, 119.

26. Rosenberg, B. *Nature* **1969**, 222, 385.

27. Canali, L.; Sherrington, D.C. *Chem. Soc. Rev.* **1999**, 28, 85.

28. Tejam, A.B.; Thakkar, N. *Indian J. Chem.* **1997**, 36(A), 1008.

29. Andrews, J.M. *J. Antimicrob. Chemother.* **2001**, 48, 5.

30. Senthilraja, P.; Kathiresan, K. *J. Appl. Pharm. Sci.* **2015**, 5, 80.

31. Vogel, A.I. *A Text Book of Quantitative Inorganic Analysis*, Longmans: London; **1975**; pp. 380 and 433.

32. Lever, A.B.P. *Inorganic Electronic Spectroscopy*, Elsevier: Amsterdam; **1984**.

33. Patil, R.M.; Prabhu, M. *Int. J. Chem. Sci.* **2010**, 68, 52.

34. Nakamoto, K. *A Text book of Infrared and Raman Spectra of Inorganic and Coordination Compound*, John Wiley and Sons: New York; **1986**.

35. Arunadevi, N.; Vairam, S. *E. J. Chem.* **2009**, 6(S$_1$), 413.

36. Adrian, H.M.; Zhang, Y.; Andrew, I.W.; Stanley Cameron, T.; Ramesh, V.; Brian J.M.; Manuel, A.S.A. *Polyhedron* **2008**, 27, 1270.

37. John, A.D. *Lange's Hand Book of Chemistry*, 15th ed., McGraw-Hill Education; New York; **1999**.

38. Siqueira, A.B,; Ionashiro, E.Y.; Carvalho, C.T.; Bannach, G.; Rodrigues, E.C.; Ionashiro M.; Massao, I. *Quim. Nova* **2007**, 30, 318.

39. Jordanovska, V.; Trojko, R. *Thermochim. Acta* **1995**, 258, 205.

40. Patil, K.C. *J. Chem. Sci.* **1986**, 96, 459.

41. Cao, G. *Nano Structures and Nano Materials, Synthesis, Properties and Applications*, Imprial College Press: London; **2004**.

42. Gehad, G.M.; Omar, M.M.; Ahmed, M.M.H. *Spectrochim. Acta Part A* **2005**, 62, 1140.

43. Amit, R.Y.; Vijaya, V.D.; Gaurav, B.P.; Anand, S.A. *Bull. Chem. Soc. Ethiop.* **2014**, 28, 255.

44. Obaleye, J.A.; Adediji, J.F.; Adebayo, M.A. *Molecules* **2011**, 16, 5861.

45. Chandraleka, S.; Ramya, K.; Chandramohan, G.; Dhanasekaran, D.; Priyadharshini, A.; Panneerselvam, A. *J. Saudi Chem. Soc.* **2014**, 8, 953.